New Journal of Physics
The open-access journal for physics

Spin-flip and spin-conserving optical transitions of the nitrogen-vacancy centre in diamond

Ph Tamarat[1], N B Manson[2], J P Harrison[2], R L McMurtrie[2], A Nizovtsev[3], C Santori[4], R G Beausoleil[4], P Neumann[1], T Gaebel[1], F Jelezko[1], P Hemmer[5] and J Wrachtrup[1]

[1] 3. Physikalisches Institut, Universität Stuttgart, 70550, Stuttgart, Germany
[2] Laser Physics Centre, Australian National University, Canberra, ACT 0200, Australia
[3] Stepanov Institute of Physics, National Academy of Sciences of Belarus, Minsk, 220072, Belarus
[4] Hewlett-Packard Laboratories, 1501 Page Mill Road, Palo Alto, CA, 94304, USA
[5] Texas A&M University, College Station, TX, 77843, USA
E-mail: j.wrachtrup@physik.uni-stuttgart.de

New Journal of Physics **10** (2008) 045004 (9pp)
Received 29 June 2007
Published 30 April 2008
Online at http://www.njp.org/
doi:10.1088/1367-2630/10/4/045004

Abstract. We map out the first excited state sublevel structure of single nitrogen-vacancy (NV) colour centres in diamond. The excited state is an orbital doublet where one branch supports an efficient cycling transition, while the other can simultaneously support fully allowed optical Raman spin-flip transitions. This is crucial for the success of many recently proposed quantum information applications of the NV defects. We further find that an external electric field can be used to completely control the optical properties of a single centre. Finally, a group theoretical model is developed that explains the observations and provides good physical understanding of the excited state structure.

The negatively charged nitrogen-vacancy (NV) centre in diamond has exceptional characteristics that make it the leading solid-state competitor to trapped ions and atoms for applications in quantum information processing and quantum storage. Yet surprisingly, details of its excited state structure have been poorly understood despite several recent impressive demonstrations of elements of scalable quantum computing with NV defects [1–5]. This knowledge is crucial for quantum information applications providing upper limits on the fidelity of the cycling transition used for spin readout. It also determines under what conditions optical Raman spin-flip transitions (which can be used to achieve direct optical control over the electron spin state) are allowed.

In this paper, we report the observation of the excited state spin sublevels in a single NV defect. In particular, we observe different excited state spin sublevels along with the variation of transition frequencies and strengths as a function of applied electric field. Using group theoretical analysis we show that it is possible to simultaneously have an efficient cycling transition and a fully allowed optical Raman spin-flip transition, as required for a high-performance quantum processor.

Impurity spins in solids in general are appealing for quantum information applications. The NV in particular offers great promise because of its paramagnetic ground state [6]–[8], and the fact that its spin can be optically polarized [9], even using broadband optical excitation at room temperature. Since the demonstrations of optical detection of single NV centres [10] and spin-selective readout [11, 12] it has been clear that this system has unique characteristics that qualify it as a solid state qubit. The recent demonstration of two-laser control of the ground state spin has significantly strengthened this prospect [12]. However, it was not clear whether it was possible to simultaneously fulfil the readout requirement for an almost perfectly cycling transition [11] and the spin-flip optical λ-type transition [12]–[14]. Previous observations suggested that these were conflicting requirements and that only one at a time could be satisfied by NV centres in very different environments.

In the present work, we resolve these issues by using multichromatic laser and microwave (MW) optical double resonance measurements to unravel the excited-state structure of single NV centres. External control using an electric field allowed us to switch between spin-state conserving and λ-type transitions. We compare the experimental observations with a group theoretical model and obtain good correspondence. The model provides the necessary insight into the excited state structure and enables us to answer questions regarding the transition type and how the transitions can be optimized. However, the work has wider implication as it leads to an improved understanding of the electronic structure of the NV centre and will enable more satisfactory development of all NV applications.

The NV defect in diamond comprises a nitrogen atom at a lattice site next to a carbon vacancy giving a centre with C_{3v} symmetry. The centre has an optically allowed transition between an orbital A_2 ground state and an orbital E excited state [15]. Both the ground and excited states are spin triplets ($S = 1$). The spin levels in the $^3A_2$ ground state are split by 2.88 GHz into a spin singlet S_z and a spin doublet (S_x, S_y). From hole burning measurements [7, 12] it is known that the ^3E excited state is likewise split by several gigahertz but the details have not been determined. At liquid helium temperature and in well chosen diamonds, the $^3A_2$–^3E spectral line widths reach their lifetime-limited value of the order of several megahertz [16]. Hence, it should be possible to establish the excited state structure from an excitation spectrum.

Note that an excitation spectrum can be influenced by spin-related properties of optical transitions. If spin–orbit and spin–spin interactions do not change the quantization axes of the

spin in the excited state, spin can be considered as a good quantum number. In this situation, we expect that the excitation spectrum of a single NV defect shows three lines corresponding to transitions between same spin sublevels of ground and excited electronic states. However, the excitation spectra of a single NV centres have given only one resonance line [11, 16] rather than the several anticipated. This can be attributed to an enhanced probability passage to a metastable singlet state for S_x, S_y states. The metastable state decays preferentially into the S_z sublevel of the ground state. The centre excited by a single laser is driven out of resonance after a few excitation–emission cycles for the S_x, S_y states, and only the S_z state shows a long-cycling transition. Therefore, the complete ^{3}E fine structure can only be obtained by a multi-frequency excitation, and this approach is realized here.

Experiments devoted to unravelling the excited state structure pose limitations on the spectral stability of NV defects. Nitrogen-rich Ib type crystals often show photoinduced spectral jumps leading to line broadening. Such spectral diffusion is possibly caused by continuous photoionization of substitutional nitrogen inducing a fluctuating electric field at the location of the NV defect. Recently, stable spectral lines were reported for ultrapure IIa type natural diamonds [16]. These IIa crystals are used in our experiments. A laser is phase-modulated to give a beam with a central frequency and sidebands at ± 2.88 GHz, such that the laser–sideband separation matches the ground spin splitting (figure 1(a)). The laser frequency was tuned to the $^3A_2$–^{3}E zero-phonon line at 637 nm and the beam was focused on a single NV defect in a type IIa diamond. Experiments were performed at cryogenic temperature ($T = 1.8$ K). The vibronic emission at 650–800 nm was detected in a confocal arrangement to obtain the excitation spectrum of single NV centres. Using modulation, spectral responses are obtained at several frequencies, whereas there are no equivalent responses in the absence of the modulation. An illustration of this situation is given by the central and lower spectra in figure 1(b). For this defect centre no fluorescence is excited when only a single laser frequency is used (see scan 13–19 in figure 1(b)). As will be explained in more detail below, for the defect centre presented an electron spin flip occurs upon optical excitation. The probability for such a spin flip depends on the details of the excited state structure which is influenced by strain or e.g. an external electric field. An electron spin flip will cause the defect centre transition not to be in resonance with the laser excitation and hence no fluorescence is excited. Fluorescence, however, is obtained when two of the optical frequencies become resonant with transitions from the two ground state spin levels to a common excited state level in a λ-type scheme. As the ground state levels are associated with distinct spin states, S_z and (S_x, S_y), there will only be allowed λ-type transitions when the excited state has a mixed spin character. The mixing occurs most efficiently between adjacent excited states and both of these mixed states will satisfy the conditions for emission. Hence, there will be two features in the sideband (SB) excitation spectrum. This is consistent with observations in figures 1(b) and 2(b) where the two resonance lines are separated by 0.32 GHz. The features are assigned to λ transitions comprising the 1 and 2 as well as 3 and 4 transitions in the energy level scheme in figure 2(a). The spectral features are repeated in the SB spectrum at an interval of 2.88 GHz when the laser and the reverse SB are resonant with the transitions. Note that this situation is rather typical for NV defects and only a small fraction of the NV defects show a long-cycling transition allowing us to observe defects without repopulating the shelving spin state by laser SBs or MW.

In a second approach MWs were applied resonant with the ground state transition at 2.88 GHz via a broad band single turn MW loop to maintain a time-averaged population within each of the ground state spin levels. The MW power applied at the input of the MW line was

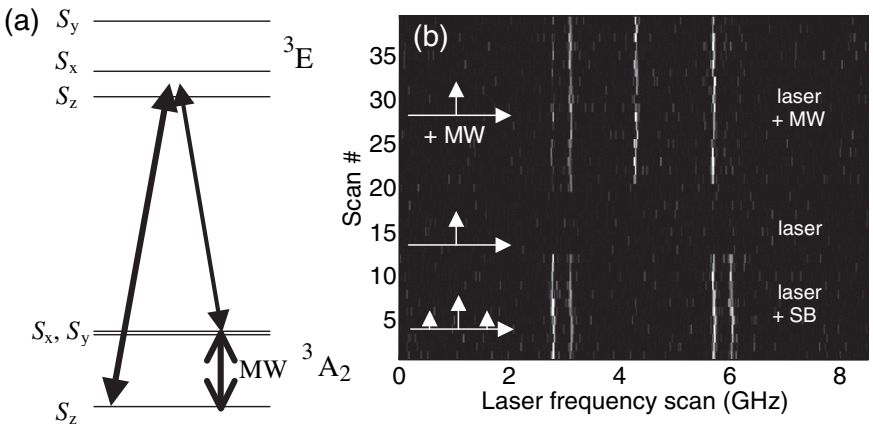

Figure 1. (a) Energy levels and laser excitation fields. (b) Spectral trails of the same NV centre when irradiated with a laser plus SBs at ±2.88 GHz (scans #1–12), with single laser (scans #13–19) and with a laser plus MWs at 2.88 GHz (scans #20 to end). Note that tuning of MW or laser SB frequency out of resonance at 2.88 GHz leads to a loss of the repumping effect (data not shown).

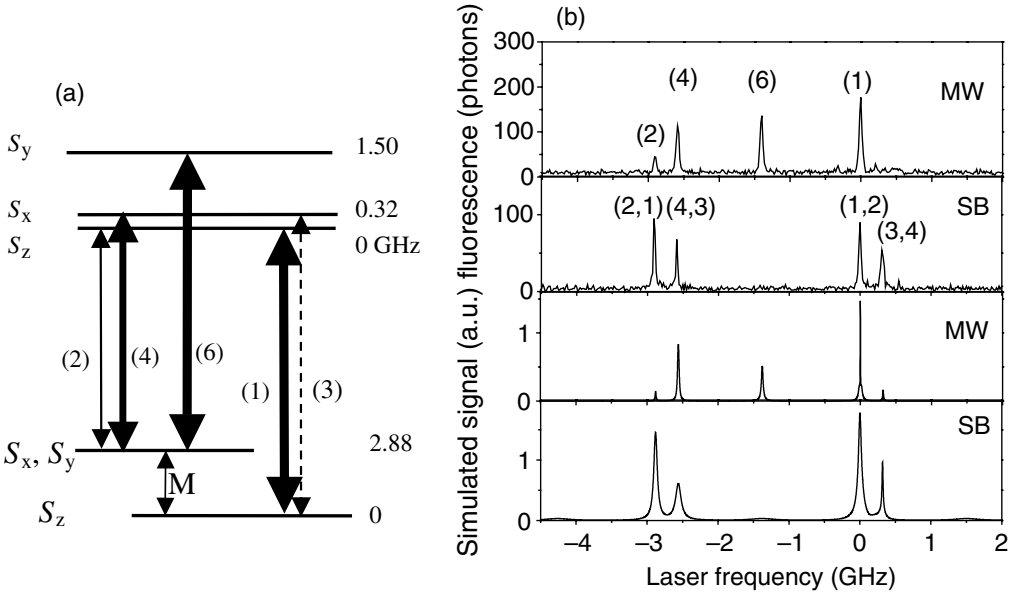

Figure 2. (a) Energy levels and assignment of transitions. (b) Spectra taken using single laser plus MWs at ±2.88 GHz (top) and using laser plus SBs (second top). In the last case, the SB frequency was set to 2.88 GHz and the laser frequency was scanned (centre of scan corresponds to laser wavelength of 637.160 nm (air)). The lower traces are obtained from simulations including optical and MW fields for a seven level model (see text).

20 dBm (100 mW). A fluorescence excitation spectrum is then recorded with a single frequency laser field. Such a spectrum is shown in the upper traces in figures 1(b) and 2(b). The transitions 1, 2 and 4 to the two excited state levels separated by 0.32 GHz are observed. An additional

transition, 6, is observed and attributed to a third excited state sublevel at 1.5 GHz (figure 2(a)). The measurements in figures 1 and 2 are interpreted in terms of transitions between three spin levels S_z, S_x and S_y in both the ground and the excited electronic state each considered to be orbital singlets. A simulation of the spectra using the six spin levels (plus an intermediate singlet level) is given in the lower traces in figure 2(b) and gives reasonable agreement with the experiments. The singlet level is necessary to account for the spin polarization in the ground state and hence for the different line intensities in figure 2(b) [9]. Note that particular splitting of excited state spin sublevels is subject to the influence of strain which is always present in the diamond lattice. Hence the energy level scheme presented in figure 2 must be considered only as an example for particular crystal strain. More general description of the excited state based on group theory analysis is presented in the last part of this paper.

There is still a need to account for the observation that only one excitation line is obtained with a single laser excitation as reported earlier [16]. This line is attributed to a different orbital level in the ^{3}E state. The ^{3}E state is an orbital doublet where the two orbital components behave differently with respect to spin state mixing. As explained below the upper branch of transitions shown in figure 3(a) is responsible for cycling transitions, i.e. where no spin flip occurs during optical excitation, while the lower branch corresponds to the situation outlined in figure 2. If this interpretation is correct, all the spectral features should be observable for a single centre and this situation is obtained in figure 3(a). The higher energy branch can be observed with a single laser and the lower one only when using a modulated laser beam.

To investigate whether the conditions of the cycling and non-cycling transitions can be controlled externally, electrodes were deposited on the ⟨001⟩ surface of the diamond to enable electric fields of up to 3 MV m^{-1} to be applied. This field has components parallel, F_z, and perpendicular, (F_x, F_y), to the axis of the NV- centre (x is defined to be in a C_{3v} reflection plane). For the latter spectrum (figure 3(a)) the electric field causes the higher energy features to be displaced with a curvature to higher energy. This is a characteristic feature that has been reported previously [16]. The lower energy features only observed using double resonance techniques have the reverse behaviour with a curvature to lower energy. The electric field also causes changes in the fine structure and typical variations are shown in figure 3(b). The changes in separations and intensities are consistent with two avoided crossings of the spin levels occurring as a function of electric field.

The observations can be explained by considering the effects on the ^{3}E state with the Hamiltonian:

$$\mathbf{H} = \mathbf{H_0} + \mathbf{H_{so}} + \mathbf{H_{elec}} + \mathbf{H_{str}}.$$

$\mathbf{H_0}$ is the dominant term and gives the energy of the state. The spin–orbit interaction $\mathbf{H_{so}}$ and the perturbations due to electric fields $\mathbf{H_{elec}}$ and strain $\mathbf{H_{str}}$ are all of the order of a few gigahertz. In C_{3v} symmetry, the S_z spin wavefunction transforms as A_2 and the associated ^{3}E spin–orbit state has $A_2 \otimes E = E$ symmetry. Spins S_x and S_y transform as rows of an E representation and the spin–orbit states have $E \otimes E = A_1, A_2$ and E symmetries. The four spin–orbit states are affected by spin–orbit interaction:

$$\mathbf{H_{so}} = \lambda(\mathbf{L_z^{(A2)}}\mathbf{S_z^{(A2)}} + \mathbf{L_x^{(E)}}\mathbf{S_x^{(E)}} + \mathbf{L_y^{(E)}}\mathbf{S_y^{(E)}}),$$

where the symmetry of the operators are given in brackets. The transverse spin–orbit interaction can lead to the mixing of spin states but the associated orbital coefficient $\lambda\langle E \parallel \mathbf{L^{(E)}} \parallel E\rangle = e$ is small and initially taken as zero such that there is no $S_z - (S_x, S_y)$ spin mixing. The wavefunctions are then determined by symmetry. Axial spin–orbit interactions $\lambda\,\mathbf{L_z^{(A2)}}\mathbf{S_z^{(A2)}}$ displace

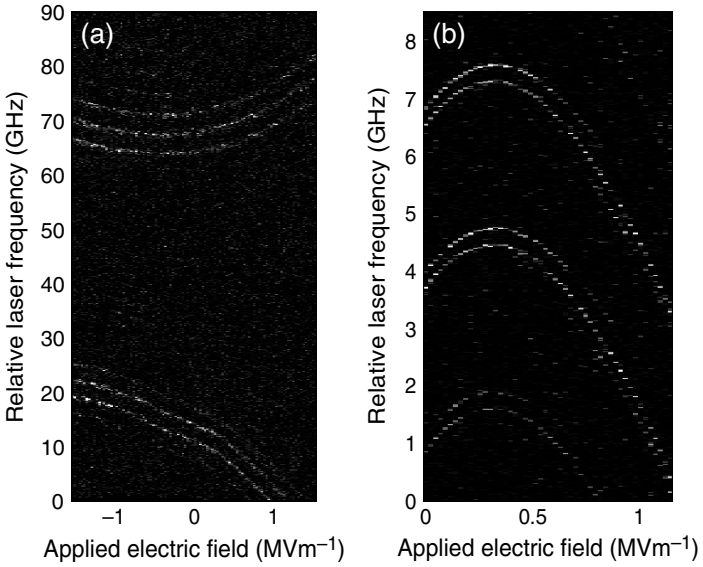

Figure 3. $^3A_2$–^3E excitation spectra as a function of external electric field. (a) Two sets of excitation lines associated with a single NV centre are obtained using a laser beam modulated at 2.88 GHz. Note that each line in the upper branch appears as a triplet related to the laser SBs. This line also can be visible in fluorescence when excited by a single laser. The lower branch appears as a doublet. This doublet structure is related to the fact that the laser having three frequency components twice matches the frequency of a λ-scheme during the scan. Spitting between two branches at zero electric field (55 GHz) corresponds to splitting of excited state related to strain present in crystal lattice. (b) The variation of the excitation spectra of a different NV centre as a function of electric field for the lower energy orbital branch.

the states associated with S_x and S_y spins $(({}^3\mathrm{E})(\mathrm{A}_1, \mathrm{A}_2))$ and $({}^3\mathrm{E})E$ by $\lambda\langle E \parallel \mathbf{L}^{(\mathbf{A2})} \parallel E\rangle = a$ and $-a$, respectively, and from a six electron (two hole) model a is considered to be positive [9]. The excited $({}^3\mathrm{E})E$ state associated with S_z spin is not displaced by spin–orbit.

The electronic model of the NV centre anticipates intermediate $^1\mathrm{A}_1$ and $^1\mathrm{E}$ singlet levels [8]. Spin–orbit interaction with $^1\mathrm{A}_1$ will cause the $({}^3\mathrm{E})\mathrm{A}_1$ state to be displaced to a higher energy by b and similarly spin–orbit interaction with the $^1\mathrm{E}$ singlet level can cause one of the $({}^3\mathrm{E})E$ states (lower) to be shifted up in energy by c. This latter shift could also arise from spin–spin interaction. The parameters a, b and c are treated as semi-empirical parameters and are estimated from experiments. The values used here are $a = 4.4$ GHz, $b = 2$ GHz and $c = 1$ GHz and these values give the zero field energy levels in figure 4(a). The electric field perturbation is given by

$$\mathbf{H}_{\mathbf{elec}} = \mathbf{F}_{\mathbf{z}}^{(\mathbf{A1})}\mathbf{D}_{\mathbf{z}}^{(\mathbf{A1})} + \mathbf{F}_{\mathbf{x}}^{(\mathbf{E})}\mathbf{D}_{\mathbf{x}}^{(\mathbf{E})} + \mathbf{F}_{\mathbf{y}}^{(\mathbf{E})}\mathbf{D}_{\mathbf{y}}^{(\mathbf{E})},$$

where $\mathbf{F}_i$ and $\mathbf{D}_i$ are the electric field and dipole operators associated with $i = z$-, x-, y-directions and the symmetries of the terms are given in brackets. The first term $\mathbf{F}_{\mathbf{z}}^{(\mathbf{A1})}\mathbf{D}_{\mathbf{z}}^{(\mathbf{A1})}$ simply gives rise to a linear shift of all levels and is not considered further. The transverse terms cause linear splittings of the orbitally degenerate E state. The splitting is independent of field direction in the xy-plane and is given by, $\pm\mu\mathrm{F} = \pm\mu\sqrt{(\mathrm{F}_x^2 + \mathrm{F}_y^2)}$, where $\mu = \langle \mathrm{E} \parallel \mathbf{D}^{(\mathbf{E})} \parallel \mathrm{E}\rangle$.

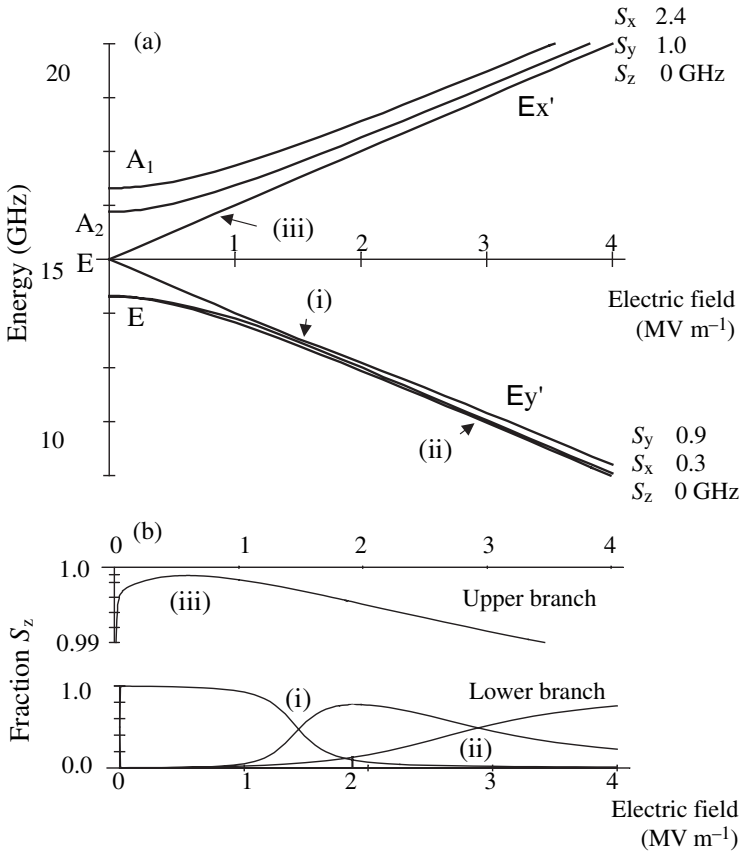

Figure 4. (a) Energy levels of the ^{3}E excited state as a function of the orbital splitting calculated for a F_y electrical field. At zero field the levels are determined by the spin–orbit parameters a, b and c given in the text. Wavefunctions are defined as $|E_{x'(y')}\rangle = |E_x\rangle \pm |E_y\rangle$ and $|S_{x'(y')}\rangle = |S_x\rangle \pm |S_y\rangle$. The values given for $S_{x,y,z}$ are relative splittings at high electric field. (b) Eigenstates giving the fraction of S_z within each state. In the upper case there is only one state with significant S_z component. Special features are labelled (i)–(iii).

From previous work μ is of the order of 6 GHz (MV m^{-1}) [16]. The orbital eigenstates vary with the direction of the electric field and for an F_x field are $|E_x\rangle$ and $|E_y\rangle$, and for a F_y field are $|E_x\rangle \pm |E_y\rangle$. The variation in the energy of the ^{3}E spin–orbit states for a field F_y applied along the y-direction is calculated numerically and shown in figure 4(a). The dominant effect is the linear splitting of the orbital components.

In the experiment, a quadratic dependence is obtained and is due to the presence of strain. This differs from the interpretation given in [14]. The terms within $\mathbf{H_{str}}$ transform as A_1 and E irreducible representations, the same as those for the electric field. Therefore, the inherent strain has the same effect as a weak electric field and the components along the z-, x- and y-directions are denoted as f_z, f_x and f_y, respectively. This allows us to define strain as an equivalent electric field. Using the example of a F_y field the splitting of the orbital levels are given by $\pm\mu\sqrt{f_x^2 + (f_y + F_y)^2}$. These quadratic variations are consistent with the observations shown in figure 3(a). The minimum separation of the two branches is determined by the

orthogonal strain field $f_x = 1\,\mathrm{MV\,m^{-1}}$ and the zero offset is determined by the parallel strain field $f_y = 0.15\,\mathrm{MV\,m^{-1}}$.

The electric field also changes the fine structure and in the upper branch the spin–orbit separations are reduced as the splitting increases (figure 4(a)). In the lower branch the state associated with S_z changes from being the highest in energy at low electric field to the lowest energy-state at high field. However, the non-axial spin–orbit interaction previously neglected can cause mixing and changing crossings to avoided crossings. In the case of a F_y field there are two avoided crossings, (i) and (ii). Setting $\lambda\langle E \parallel L \parallel E\rangle = e = 0.2\,\mathrm{GHz}$ the calculated variation shown in figure 4(a) is in good correspondence with the experimental situation of figure 3(b).

To give a comprehensive picture of our findings in terms of spin conserving (cycling) versus spin flip (λ) transitions, in figure 4(b) we have plotted the spin projections of the calculated eigenfunctions on to the S_z state. The lowest trace shows the mixing of the basis states in the region of the two avoided crossings ((i) and (ii) in figure 4(b)). The variation of mixing is consistent with the observations in the two-laser experiment (figure 3(b)). Thus, as also shown by the experiments, the lower branch will, in general, show non-cycling transitions, i.e. will not be observable with single laser excitation. This is the case for the defect centre shown in figure 2 (see traces 13–19). The lower branch in figure 4(a) thus also corresponds to the lower branches of transition energies in figures 3(a) and (b). The situation with the upper branch is totally different. In this case the S_z spin level is not susceptible to spin mixing (figure 4(b)). For a small electric field there is less than 1 in 10^3 component of (S_x, S_y) spins at (iii) and the mixing remains small over the range of electric fields calculated. Transition from the S_z ground level to this upper branch level is long-cycling. Hence, it can be observed in a single laser excitation spectrum. Also as there is no $(S_x, S_y) - \mathrm{S}_z$ mixing the levels will not be observed in the two-frequency optical experiments. It is concluded that the model gives good correspondence with all of the characteristics observed experimentally.

The model allows us to comment on other issues. For example, we note that an external electric field has similar effects on the optical properties of the defect centre to naturally occurring strain. The cyclic (i.e. spin state conserving) transitions are optimal at low but nonzero field (figure 4(b)) and can occur when there is a λ transition associated with the lower orbital branch. This gives a positive answer to the question of whether cyclic- and λ-transitions can occur simultaneously for a single NV centre. Note that by varying the field one transition type can be optimized but the other transition is degraded. It is also possible to anticipate the degree of spin polarization for different situations. As can be seen from figure 4(b) it depends on whether one is close to an avoided crossing in the lower branch of the excited state.

The present work has provided significant insight into the ^{3}E excited state of the NV centre. This is invaluable for the development of applications for the NV centre but in particular for its use in quantum information processing. A well controlled single spin readout and all-optical control of single electrons and probably even single nuclear spins is within reach. Moreover this study demonstrates that for the NV centre the relative strength of spin flip versus spin allowed optical transitions can be tuned by an external control parameter. It also highlights the importance of local strain for spectroscopy of NV defects. This might be of particular importance for quantum memory and repeater schemes [17] where efficient photon to spin state conversion is of importance.

Acknowledgments

The work is supported by QAP, NEDQIT and EQUIND grants from the European Commission, a SFB/TR 21 grant from DFG, Atomoptik grant from Landesstiftung BW, QuIST support from DARPA, DARPA and the Air Force Office of Scientific Research through AFOSR contract no. FA9550-05-C-0017, and grants from the Australian Research Council and DSTO. Ph T acknowledges the Alexander von Humboldt Foundation for a research fellowship.

References

[1] Childress L, Dutt M V G, Taylor J M, Zibrov A S, Jelezko F, Wrachtrup J, Hemmer P R and Lukin M D 2006 Coherent dynamics of coupled electron and nuclear spin qubits in diamond *Science* **314** 281–5
[2] Jelezko F, Gaebel T, Popa I, Domhan M, Gruber A and Wrachtrup J 2004 Observation of coherent oscillation of a single nuclear spin and realization of a two-qubit conditional quantum gate *Phys. Rev. Lett.* **93** 130501
[3] Hanson R, Mendoza F M, Epstein R J and Awschalom D D 2006 Polarization and readout of coupled single spins in diamond *Phys. Rev. Lett.* **97** 087601
[4] Dutt M V G, Childress L, Jiang L, Togan E, Maze J, Jelezko F, Zibrov A S, Hemmer P R and Lukin M D 2007 Quantum register based on individual electronic and nuclear spin qubits in diamond *Science* **316** 1312–6
[5] Gaebel T *et al* 2006 Room-temperature coherent coupling of single spins in diamond *Nat. Phys.* **2** 408–13
[6] Loubser J and Vanwyk J A 1978 Electron-spin resonance in study of diamond *Rep. Prog. Phys.* **41** 1201–48
[7] Reddy N R S, Manson N B and Krausz E R 1987 2-Laser spectral hole burning in a color centre in diamond *J. Lumin.* **38** 46–7
[8] Redman D A, Brown S, Sands R H and Rand S C 1991 Spin dynamics and electronic states of N-V centers in diamond by EPR and 4-wave-mixing spectroscopy *Phys. Rev. Lett.* **67** 3420–3
[9] Manson N B, Harrison J P and Sellars M J 2006 Nitrogen-vacancy centre in diamond: model of the electronic structure and associated dynamics *Phys. Rev.* B **74** 104303
[10] Gruber A, Drabenstedt A, Tietz C, Fleury L, Wrachtrup J and vonBorczyskowski C 1997 Scanning confocal optical microscopy and magnetic resonance on single defect centres *Science* **276** 2012–4
[11] Jelezko F, Popa I, Gruber A, Tietz C, Wrachtrup J, Nizovtsev A and Kilin S 2002 Single spin states in a defect centre resolved by optical spectroscopy *Appl. Phys. Lett.* **81** 2160–2
[12] Santori C *et al* 2006 Coherent population trapping in diamond N-V centres at zero magnetic field *Opt. Express* **14** 7986–93
[13] Santori C *et al* 2006 Coherent population trapping of single spins in diamond under optical excitation *Phys. Rev. Lett.* **97** 247401
[14] Hemmer P R, Turukhin A V, Shahriar M S and Musser J A 2001 Raman-excited spin coherences in nitrogen-vacancy color centres in diamond *Opt. Lett.* **26** 361–3
[15] Davies G and Hamer M F 1976 Optical studies of 1.945 eV vibronic band in diamond *Proc. R. Soc. Lond.* A **348** 285–98
[16] Tamarat P *et al* 2006 Stark shift control of single optical centres in diamond *Phys. Rev. Lett.* **97** 083002
[17] Childress L, Taylor J M, Sorensen A S and Lukin M D 2006 Fault-tolerant quantum communication based on solid-state photon emitters *Phys. Rev. Lett.* **96** 070504